Received: 28 January 2018 | Revised: 15 August 2018 | Accepted: 30 August 2018

DOI: 10.1002/hbm.24390

WILEY

RESEARCH ARTICLE

White matter network connectivity deficits in developmental dyslexia

Chenglin Lou[1] | Xiting Duan[1] | Irene Altarelli[2,3] | John A. Sweeney[4] | Franck Ramus[2] | Jingjing Zhao[1]

[1]School of Psychology, Shaanxi Normal University, and Key Laboratory for Behavior and Cognitive Neuroscience of Shaanxi Province, Xi'an, China

[2]Laboratoire de Sciences Cognitives et Psycholinguistique (ENS, EHESS, CNRS), Département d'Etudes Cognitives, Ecole Normale Supérieure, PSL Research University, Paris, France

[3]Faculty Psychology and Science De L'éducation (FPSE), University of Geneva, Geneva, Switzerland

[4]Department of Psychiatry and Behavioral Neuroscience, University of Cincinnati, Cincinnati, Ohio

Correspondence
Jingjing Zhao, School of Psychology, Shaanxi Normal University, 199 South Chang'an Road, Xi'an 710062, China.
Email: jingjing.zhao@snnu.edu.cn

Funding information
Agence Nationale de la Recherche, Grant/Award Numbers: ANR-11-0001-02 PSL∗, ANR-10-LABX-0087, ANR-11-BSV4-014-01, ANR-06-NEURO-019-01; the Fundamental Research Funds for the Central Universities, Grant/Award Number: GK201702011; the General Project (Youth) of Shaanxi Natural Science Basic Research Program, Grant/Award Number: 2018JQ8015; the Youth Fund for Humanities and Social Sciences Research of the Ministry of Education, Grant/Award Number: 17XJC190010

Abstract

A number of studies have shown an abnormal connectivity of certain white matter pathways in developmental dyslexia, as well as correlations between these white matter pathways and behavioral deficits. However, whether developmental dyslexia presents broader white matter network connectivity disruption is currently unknown. The present study reconstructed white matter networks for 26 dyslexic children (11.61 ± 1.31 years) and 31 age-matched controls (11.49 ± 1.36 years) using constrained spherical deconvolution tractography. Network-based statistics (NBS) analysis was performed to identify network connectivity deficits in dyslexic individuals. Network topological features were measured based on graph theory to examine whether these parameters correlate with literacy skills, and whether they explain additional variance over previously established white matter connectivity abnormalities in dyslexic children. The NBS analysis identified a network connecting the left-occipital-temporal cortex and temporo-parietal cortex that had decreased streamlines in dyslexic children. Four network topological parameters (clustering coefficient, local efficiency, transitivity, and global efficiency) were positively correlated with literacy skills of dyslexic children, and explained a substantial proportion of additional variance in literacy skills beyond connectivity measures of white matter pathways. This study for the first time reports a disconnection in a local subnetwork in the left hemisphere in dyslexia and shows that the global white matter network topological properties contribute to reduced literacy skills in dyslexic children.

KEYWORDS

dyslexia, graph theory, literacy, NBS, white matter network

1 | INTRODUCTION

Developmental dyslexia is characterized by difficulty in learning to read that is independent from intelligence (Lyon, Shaywitz, & Shaywitz, 2003). This disorder has a population prevalence of 5%–10% (Shaywitz, Shaywitz, Fletcher, & Escobar, 1990; Siegel, 2006) and is recognized to have a neurobiological origin (Fawcett & Nicolson, 2007). Developing a more comprehensive understanding of the neurological basis of developmental dyslexia and establishing its clinical relationship with reading deficits remains a primary aim of dyslexic research (Giraud & Ramus, 2013).

It is widely accepted that reading involves multiple brain regions, including the frontal lobe, parieto-temporal regions and occipito-temporal regions (Epelbaum et al., 2008; Hoeft et al., 2006; Hoeft et al., 2007; Shaywitz & Shaywitz, 2005). Compared to typical readers, people with dyslexia normally exhibit an atypical pattern of brain

activity across distributed brain regions (Brambati et al., 2006; Cohen et al., 2000; Cohen & Dehaene, 2004; Dehaene & Cohen, 2011; Paulesu, Danelli, & Berlingeri, 2014; Price & Devlin, 2011; Shaywitz et al., 2002) as well as abnormal functional connectivity among reading-related brain regions (Boets et al., 2013; Horwithz, Rumsey, & Donohue, 1998; Paulesu et al., 1996; Pugh et al., 2000; Schurz et al., 2015; Zhou, Xia, Bi, & Shu, 2015).

Functional connectivity deficits found in dyslexia may result from white matter connectivity alterations, as white matter fiber bundles connect distant brain regions and ensure long-range connections between brain regions. Diffusion tensor imaging (DTI) provides a non-invasive way to measure the connectivity of white matter fiber tracts by calculating the diffusion tensor within each voxel to estimate orientations and integrity of white matter fibers (Basser, 1995; Basser, Mattiello, & Lebihan, 1994). White matter integrity has been found to be decreased in various white matter structures in dyslexia compared with typically developing controls (Deutsch et al., 2005; Klingberg et al., 2000; Niogi & McCandliss, 2006; Richards et al., 2008; Rimrodt et al., 2009; Steinbrink et al., 2008), especially in the left arcuate fasciculus, a fiber pathways connecting Broca's area and Wernicke's area (Catani & Thiebaut de Schotten, 2008; Vandermosten, Boets, Poelmans, et al., 2012; Zhao, Thiebaut de Schotten, Altarelli, Dubois, & Ramus, 2016).

While previous studies have performed whole-brain analysis (e.g., TBSS) to identify local differences in white matter connectivity in dyslexia since last decades, whole-brain network analysis methods (e.g., network-based statistic [NBS] and graph theory analysis) have only been used to examine local and global network deficits in dyslexia recently. These included one study with functional connectivity network analysis (Finn et al., 2014) and two studies with gray matter network analysis (Hosseini et al., 2013; Qi et al., 2016). Finn et al. reported an altered local visual network in dyslexia using whole-brain functional network analysis method (NBS), suggesting that dyslexia may result from reduced functional synchronization among occipital regions (Finn et al., 2014). Whole-brain gray matter network analyses found altered network properties in cortical thickness and surface area in dyslexia (Qi et al., 2016) and in children with familial risk of dyslexia (Hosseini et al., 2013) using graph theory analysis method. However, no study has examined white matter network deficits in dyslexia. It remains unknown whether anomalies in white matter connectivity might be reflected at a global network level.

The purpose of the present study was to evaluate whether developmental dyslexia has anatomic connectivity deficits at the whole-brain network level by using white matter network analysis methods (NBS and graph theory analysis). Network analysis expands analysis of white matter connectivity from investigations of specific pathways to an entire connectome analysis. By mapping the brain as a network composed of nodes and edges, network-based analysis methods have been successfully used to quantify the connectivity of brain networks in clinical populations with neurological and psychiatric disorders such as autism (Roine et al., 2015), major depressive disorder (Korgaonkar, Fornito, Williams, & Grieve, 2014), preterm born infants and children (Ball et al., 2014; Batalle et al., 2017), and Alzheimer's disease (Reijmer et al., 2013; Wang et al., 2015) [for a review see Sporns, 2014].

The specific aims of the present study are threefold: (1) to evaluate whether there are white matter network connection deficits in developmental dyslexia using network-based statistic; (2) to explore whether there are deficits in the network topological properties of white matter networks in dyslexia by graph theory analysis; and (3) to examine whether there is a correlation between the topological properties and the severity of reading disability in dyslexia, and whether those topological parameters might explain additional behavioral variance in literacy skills over and above already established white matter pathway disruptions in dyslexia.

2 | METHODS AND MATERIALS

2.1 | Participants

Fifty-seven children were enrolled into the study. Twenty-six children were dyslexic (11.61 ± 1.31 years) and the other 31 children were typical readers (11.49 ± 1.36 years). The age of children ranged from 109 to 169 months (9 to 14 years). All children were French native speakers with normal vision and hearing abilities, and their nonverbal IQ were all higher than 80. Dyslexic children were all severe dyslexic participants diagnosed at a clinic for reading and language disabilities, had no history of brain damage, and were screened for ADHD using the appropriate subscale of the Child behavior checklist (Achenbach, 2001). Text reading age [based on accuracy and speed of the Alouette test (Lefavrais, 1967)] was delayed by at least 18 months for dyslexic children and no more than 12 months for controls. Age, sex, handedness, maternal educational level, and nonverbal IQ were matched across groups. We used the 18-month delay criterion to make sure that these dyslexic children were all very poor readers at the time of scanning. Informed written consent was obtained from all children and their parents, and the study was approved by the ethics committee of Bicêtre Hospital, France. A previous analysis of certain white matter pathways in these participants has been published, and no difference in head motion parameters was found between dyslexics and controls (Zhao et al., 2016).

2.2 | Behavioral measures

Intellectual abilities were tested using the WISC blocks, matrices, similarities, and comprehension subtests (Wechsler, 2005). The Alouette test (Lefavrais, 1967), which assessed reading accuracy and speed using a meaningless text, and a word/nonword reading fluency test from Odedys (Jacquier-Roux, Valdois, & Zorman, 2005) were administered to estimate children's reading ability. Orthographic skill was estimated by a word spelling-to-dictation test (Martinet & Valdois, 1999). A phoneme deletion task (Sprenger-Charolles, Béchennec, Colé, & Kipffer-Piquard, 2005), a spoonerism test (Bosse & Valdois, 2009), and the WISC digit span subtest assessing verbal working memory (Wechsler, 2005) were administered to measure phonological skills. The rapid automatized naming (RAN) tasks for digits and objects (Plaza & Robert-Jahier, 2006) were administered to assess rapid lexical retrieval. Parental education was based on the highest diploma obtained and was coded on a scale ranging from 1 to 6. Based on a previous factor analysis of the same set of variables in a larger population from which this sample was drawn (Saksida et al., 2016), behavioral measurements were collapsed into

three factors: literacy skill (average *z*-score of word reading accuracy and word spelling accuracy), phonological ability (average *z*-score of phoneme deletion, spoonerism, and digit span), and rapid automatic naming (average *z*-score of objects rapid automatic naming and digits rapid automatic naming).

2.3 | Imaging acquisition

All children were familiarized with the scanner environment in a mock MRI setup and then underwent scanning with a 3T MRI system (Tim Trio, Siemens Medical Systems, Erlangen, Germany) equipped with a whole body gradient (40 m T/m, 200 T/m/s) and 32-channel head coil, at the Neurospin centre, Gif-sur-Yvette, France. Whole-brain anatomic imaging was performed using a MPRAGE sequence (acquisition matrix = 230 × 230 × 224, repetition time (TR) = 2,300 ms, echo time (TE) = 3.05 ms, flip angle = 9°, field of view (FOV) = 230 mm, voxel size = 0.9 × 0.9 × 0.9 mm^3).

For diffusion weighted imaging, to reduce geometric distortions, the procedure used a diffusion-weighted spin-echo single-shot EPI sequence with parallel imaging (GRAPPA reduction factor 2), partial Fourier sampling (factor 6/8), and bipolar diffusion gradients. The whole brain was imaged with an isotropic spatial resolution of 1.7 mm^3 (matrix size = 128 × 128, FOV = 218 mm) and 70 interleaved axial slices. Diffusion gradients were applied along 60 orientations, uniformly distributed, with a diffusion weighting of b = 1,400 s/mm^2 (TR = 14,000 ms, TE = 91 ms). To make this protocol tolerable for children, three subsequences were acquired separately with 20, 21, and 19 diffusion weighted (DW) volumes (Dubois, Poupon, Lethimonnier, & Bihan, 2006), in which gradient orientations were as uniformly distributed as possible in space. Additionally, three b0 images were acquired with no diffusion gradient applied (b = 0), one per run. Each sequence took about 6 min, resulting in a total acquisition time of 18 min.

2.4 | Image analysis

All the steps for image analysis, except for atlas registration, were performed using ExploreDTI (http://www.exploredti.com, see Leemans, Jeurissen, Sijbers, & Jones, 2009). For each of the 57 children, volumes from the three scans were first concatenated into a single 4D image set. Coregistration and eddy current correction were applied on the resultant 4D images to correct for subject motion and geometric distortions. Next, the b0 images of each participant were exported from each DW data set. To optimize the quality of the registration results, the voxel size of the b0 image was resampled from 1.7 × 1.7 × 1.7 mm^3 to 1 × 1 × 1 mm^3 matching the voxel size of the Automated Anatomical Labeling (AAL) template (Tzourio-Mazoyer et al., 2002). Constrained spherical deconvolution (CSD) was used to estimate multiple fiber orientations with whole-brain tractography conducted in native space (Tournier, Calamante, & Connelly, 2007). Fibers were reconstructed by starting seed samples uniformly throughout the data at 1.7 mm isotropic resolution and by following the main diffusion direction (as defined by the principal eigenvector) until the fiber tract made a high angular turn considered to be anatomically unlikely (angle <35°). The step size was set at 0.5 mm. The fiber length range was between 25 mm and 500 mm (Zhao et al., 2016).

Network construction included two types of elements—nodes and edges. In a white matter network, nodes represent cortical regions and edges correspond to white matter fiber pathways connecting cortical regions.

Node definition for each participant was based on the AAL template. According to the AAL atlas, the whole-brain gray matter (excluding cerebellum) of each child was divided into 90 regions of interest (ROIs). First, the b0 image of each participant was registered to the T1 image, generating a transfer matrix. Then the T1 image was registered to the MNI152 (Montreal Neurological Institute) template to perform a nonlinear registration. After combining those two transformations, which moved the images from native space to standard space, the inverse transformation was calculated and applied to the atlas in standard space to project back to the individual native space. All these steps were executed using FMRIB's Nonlinear Image Registration Tool (FNIRT, FSL, http://www.fmrib.ox.ac.uk/fsl/) (Jenkinson, Beckmann, Behrens, Woolrich, & Smith, 2012).

Edges were defined as the white matter fibers connecting each pair of nodes, representing white matter pathways between two gray matter regions. In a weighted network, each edge is valued to represent a connection property between two nodes. Number-of-streamlines weighted and density-weighted networks were both constructed in the present study. The value of edges in the number-of-streamlines weighted network was equal to the total number of streamlines between the two nodes connected by the edge. The value of edges in the density-weighted network was calculated by dividing the total number of streamlines between two nodes by the total surface area of the two nodes. Figure 1 illustrates the application of the AAL template to each brain, the whole-brain constrained spherical deconvolution tractography, and the edges and nodes identified in the density-weighted white matter network.

2.5 | Network-based statistic analysis

Network-based statistic (NBS) analysis is a statistical approach used to identify group differences in network organization (Zalesky, Fornito, & Bullmore, 2010). NBS was applied to both the number-of-streamlines and density weighted networks. First, group differences in each connection (streamline number or density) were examined based on a one-tail *t* test with contrast setting as "[−1, 1]" to examine, if there are subnetworks with lower connectivity in the dyslexic group than the control group. Following the trial and error progress in NBS, a series of alpha value was used to construct a set of suprathreshold links. Components were defined as sets of interconnected suprathreshold links, identified using a breadth first search (Ahuja, Magnanti, & Orlin, 1993) and characterized by their size, that is, the number of links they contained. To ascribe a *p* value controlled for the family-wise error (FWE) rate to each component, permutation testing was conducted based on each component's size. Five thousand permutations of group membership were generated independently. After applying the same threshold of alpha value to each permuted network, the maximal component size in the suprathreshold links was stored, yielding an empirical estimate of the null distribution of maximal component size. Finally, the empirical

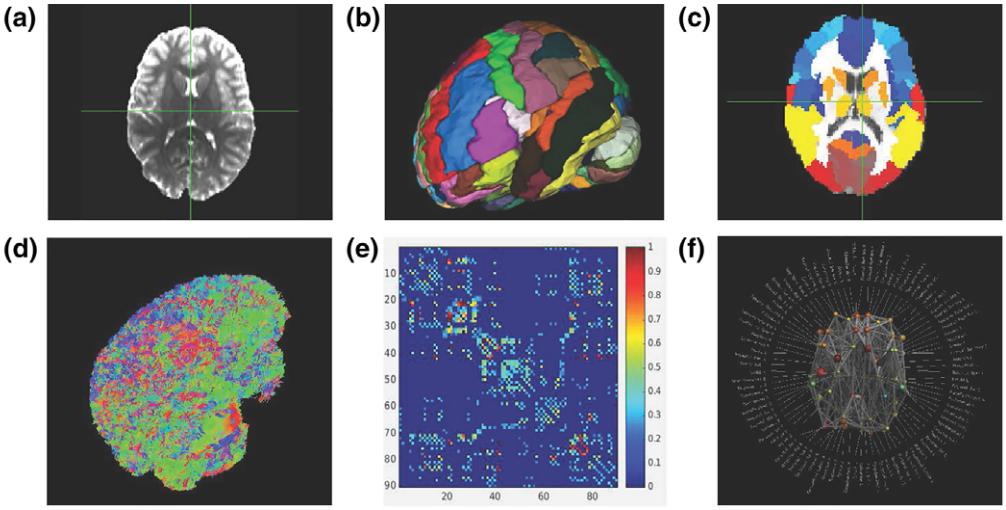

FIGURE 1 Workflow of method for constructing a whole-brain white matter network: The b0 image was exported from DW data set and then resampled to 1 × 1 × 1 mm^3 (a); the automated anatomical labeling (AAL) template (b) in standard space was registered into the b0 images of each participant in native space (c); whole-brain tractography (d) was conducted using constrained spherical deconvolution (CSD) algorithm and coregistered to the AAL template in native space generating a density weighted connection matrix between the 90 AAL cortical regions (e) which represents a whole-brain white matter network (f)

p value of the observed component of size *k* was estimated by finding the number of permutations for which the maximal component size is greater than *k* and normalizing by 5,000. This analysis was done once on the number-of-streamlines weighted network, and once on the density-weighted network. In the present study, the FWE rate for component size was set at 0.025. The visualization of the subgraphs was performed using BrainNet Viewer (http://www.nitrc.org/projects/bnv/) (Xia, Wang, & He, 2013).

2.6 | Graph theory analysis

To investigate topological properties of white matter networks, a set of thresholds were set to avoid false positive connections and keep the number of edges equal among all participants, to eliminate confounding factors such as different number of edges and connected nodes which may induce spurious group differences (Drakesmith et al., 2015; Meunier, Achard, Morcom, & Bullmore, 2009; van den Heuvel et al., 2009). The set of thresholds ranged from 10% to 30% with a step size of 1%, preserving the strongest connections (Korgaonkar et al., 2014). This range of thresholds is usually used to obtain a network with small-world properties (Korgaonkar et al., 2014; Zhang et al., 2011). We tested small-worldness at each threshold value, using the following approach (Humphries & Gurney, 2008):

$$S = \frac{C/C_{\text{rand}}}{L/L_{\text{rand}}},$$

where C and C_{rand} are the clustering coefficient (see definition below), and L and L_{rand} are the characteristic path length of the target network and of a random network.

$$L = \frac{1}{n}\sum_{i\in N}\frac{\sum_{j\in N, j\neq 1} d_{ij}}{n-1},$$

where d_{ij} is the shortest-path length between node *i* and *j*. A network is said to be small-world when small-worldness parameter $S > 1$. For each threshold between 10% and 30%, we computed the *S* value of networks across thresholds from 10% to 30% to check whether our data met that property. One sample *t* tests were applied to examine whether the *S* value was significantly higher than 1 across all thresholds. Results were corrected for multiple tests with Bonferroni correction.

Subsequent analyses were then carried out only at those thresholds in accordance with small-worldness. Six parameters (clustering coefficient, local efficiency, global efficiency, transitivity, betweenness centrality, strength) were chosen to evaluate group differences in topological properties, based on both number-of-streamlines weighted and density-weighted networks. All parameters were extracted using Brain Connectome Toolbox (Rubinov & Sporns, 2010, https://sites.google.com/site/bctnet/). Clustering coefficient (CC) measures the prevalence of clustered connectivity around each node (Watts & Strogatz, 1998). Higher average CC in the whole network indicates that there are more clusters, with all nodes more densely connected with each other.

$$CC = \frac{1}{n}\sum_{i\in N}\frac{2t_i}{k_i(k_i-1)},$$

where t_i is the number of triangles around node *i*, and k_i is the degree of a node *i* (the number of nodes directly connected with node *i*).

Efficiency has been widely used in complex network analysis to evaluate parallel information processing (Latora & Marchiori, 2001). Specifically, local efficiency (*LE*) is the average efficiency of local subgraphs formed by the neighborhood of a node, representing the fault tolerant capacity of the network when a random node lesion occurs (Latora & Marchiori, 2001).

$$LE = \frac{1}{n}\sum_{i\in N}\frac{\sum_{j,h\in N, j\neq 1} a_{ij}a_{ih}\left[d_{jh}(N_i)\right]^{-1}}{k_i(k_i-1)},$$

where a_{ij} is the value of connection between node *i* and *j*. Global efficiency (*GE*) measures the information transferring ability of whole

brain evaluated by previously established procedures (Latora & Marchiori, 2001).

$$GE = \frac{1}{n}\sum_{i\in N}\frac{\sum_{j\in N, j\neq 1} d_{ij}}{n-1}.$$

Transitivity (T) is a variant of the clustering coefficient that is computed on a global level rather than averaging the value of each node, ensuring resilience by disproportionately weighing low-degree nodes.

$$T = \frac{\sum_{i\in N} 2t_i}{\sum_{i\in N} k_i(k_i-1)}.$$

Betweenness centrality (BC) is the fraction of all shortest paths in the network that contain a given node.

$$BC = \frac{1}{(n-1)(n-2)}\sum_{h,j\in N}\frac{\rho_{hj}(i)}{\rho_{hj}},$$

where $\rho_{hj}(i)$ is the number of shortest path lengths between node h and j that pass through node i. Strength (S) is the average of all nodes' strength S_i, the number of links connected to the node i.

$$S_i = \sum_{j\in N} a_{ij}.$$

2.7 | Statistical analysis of graph theory measures

To investigate group differences of network topological properties (CC, LE, GE, T, BC, S), a multivariate analysis of covariance (MANCOVA) was performed with group (control vs. dyslexic) as a between-subject variable, and age, gender and parental education as covariates. CC, LE, GE, T, BC and S across all thresholds following small-worldness were entered into the model as dependent variables for number-of-streamline and density weighted network, separately. Correction for multiple tests (6 network topological properties × 2 weighting methods) used the False Discovery Rate (FDR) correction (Benjamini & Hochberg, 1995). Tests of partial correlations between network parameters and three behavioral composite measurements were then conducted within the dyslexic group, controlling for sex, age, parental education and mean global FA, using FDR to correct for multiple comparisons.

Network topological parameters which were significantly correlated with behavioral measurements were then entered in hierarchical multiple regression analyses to examine their additional value to predict reading dysfunction in developmental dyslexia, beyond that of previously identified white matter tract integrity measures which have been found to correlate with literacy skills using the same sample (Zhao et al., 2016). The behavioral measurements were the dependent variables. The following parameters were entered as independent variables: model 1: gender, age, parental education, and mean global FA; model 2: model 1 + the lateralization index (LI) of the inferior fronto-occipital fasciculus (IFOF) and the superior longitudinal fasciculus (SLF) II which have been shown to be significantly correlated with reading/spelling accuracy in dyslexic children (data from previous study using the same sample) (Zhao et al., 2016); model 3: model 2 + network topological parameters. The additional share of variance explained (ΔR^2) between the model and the previous model and the corresponding p value was calculated. Because of multicollinearity (condition index >30, VIF > 10), clustering coefficient, local efficiency, global efficiency, and transitivity were entered into the model and analyzed separately.

3 | RESULTS

3.1 | Demographic and behavioral measures

Descriptive statistics for demographic and behavioral measures for the dyslexic and control groups are shown in Table 1. Age, gender, handedness, nonverbal IQ and maternal education did not differ between groups. Literacy, phonological abilities, and rapid naming speed were significantly lower in the dyslexic than in the control group. Dyslexic children also had lower verbal IQ scores than controls.

3.2 | Small-worldness properties

Small-worldness parameters (S) across thresholds from 10% to 30% in the density weighted network and in the number-of-streamline weighted network were all higher than one (Table 2). However, only thresholds from 12% to 26% survived Bonferroni correction.

3.3 | Network-based statistics

For number-of-streamline network, a component network in the left occipito-temporo-parietal region whose connections were significantly weaker (FWE corrected p = .023) in dyslexic children compared with controls (Figures 2 and 3) was identified when the alpha value was .0055. The subgraph comprised seven edges connecting eight brain nodes, including the connections between left middle temporal gyrus (MTG.L) and left middle occipital gyrus (MOG.L), MOG.L and left temporal pole (TPOsup.L), TPOsup.L and left Heschl's gyrus (HES.L), HES.L and left Rolandic operculum (ROL.L), left insula (INS.L) and ROL.L, left superior temporal gyrus (STG.L) and INS.L, and between INS.L and left supramarginal gyrus (SMG.L). As a follow-up to facilitate the interpretation of this finding, all FA value of the seven edges were extracted and averaged as the mean FA of the subnetwork. We found that the mean FA of this subnetwork was significantly lower in dyslexic children compared with controls ($F_{(1, 55)}$ = 6.935, p = .011). The analysis based on the density-weighted network did not yield any component that significantly differed between groups.

For examining if the NBS results we have reported could be replicated using different node and edge definitions, we performed further validation analyses using fiber orientation distribution (FOD) as an alternative edge definition and the Harvard-Oxford 96-regions atlas (Makris et al., 2006) as an alternative node definition. All procedures and results are listed in the Supporting Information.

3.4 | Graph theory analysis

Results from the MANOVA showed that CC, LE, T, GE, BC, and S had no significant group differences between dyslexic and control group neither in number-of-streamline nor density weighted networks (ps > .1). Correlations between the mean value for each of the six network parameters across thresholds from 12% to 26% (threshold following

TABLE 1 Demographical data, behavioral scores, and brain measurements

	Control children		Dyslexic children		Test statistics
	N	Mean (*SD*)	N	Mean (*SD*)	
Subject characteristics					
Gender (male/female)	31	18/13	26	13/13	χ^2 (1) = .371, p = .543
Handedness (left/right)	31	2/29	26	3/23	χ^2 (1) = .457, p = .499
Age (years)	31	11.49 (1.36)	26	11.61(1.31)	t (55) = −.320, p = .751
Maternal education	31	2.65 (1.38)	26	3.08 (1.80)	t (55) = −1.029, p = .308
Paternal education	31	2.52 (1.61)	26	3.62 (1.92)	t (55) = −2.352, p = .022
Nonverbal IQ	31	110.29 (17.09)	26	106.00 (15.69)	t (55) = .980, p = .332
Verbal IQ	31	123.84 (18.70)	26	107.88 (18.22)	t (55) = 3.246, p = .002
Reading age (months)	31	145.94 (18.65)	26	87.27 (11.43)	t (55) = 13.979, p < .0001
Behavioral tests					
Word reading accuracy (/20)	31	18.65 (1.64)	25	10.52 (4.33)	t (54) = 9.650, p < .0001
Spelling (%)	31	82.75 (13.77)	26	37.94 (20.18)	t (55) = 9.922, p < .0001
Phoneme deletion (/24)	31	22.97 (1.38)	26	17.89 (4.77)	t (55) = 5.667, p < .0001
Spoonerism (/12)	31	7.83 (2.56)	24	2.29 (2.73)	t (53) = 7.679, p < .0001
Digit span (WISC scaled score)	31	10.87 (2.68)	26	6.58 (2.18)	t (55) = 6.554, p < .0001
RAN digits (s)	31	21.33 (3.19)	26	32.60 (7.62)	t (55) = −7.493, p < .0001
RAN objects (s)	31	35.86 (6.92)	26	51.23(9.52)	t (55) = −7.043, p < .0001
Brain measurements					
Mean global fractional anisotropy	31	.474 (.012)	26	.473 (.016)	t (55) = .249, p = .804
Head motion parameter	31	4.239 (1.378)	26	4.936 (2.413)	t (55) = −1.365, p = .178

TABLE 2 Small-worldness across thresholds from 0.10 to 0.30 on both density and number-of-streamline weighted network

Thresholds	Density weighted network			Number-of-streamline weighted network		
	Mean	*SD*	*p*	Mean	*SD*	*p*
.10	1.0349	.20476	.203	1.0345	.20413	.207
.11	1.0703	.21538	.017	1.0708	.21538	.016
.12	1.1087	.21385	<.001	1.1091	.21495	<.001
.13	1.1361	.21393	<.001	1.1372	.21540	<.001
.14	1.1739	.22147	<.001	1.1741	.22200	<.001
.15	1.2072	.22829	<.001	1.2080	.22812	<.001
.16	1.2445	.23488	<.001	1.2447	.23507	<.001
.17	1.2831	.24627	<.001	1.2839	.24679	<.001
.18	1.3174	.25757	<.001	1.3176	.25570	<.001
.19	1.3542	.25692	<.001	1.3544	.25777	<.001
.20	1.3826	.26268	<.001	1.3820	.26217	<.001
.21	1.4179	.27514	<.001	1.4163	.27328	<.001
.22	1.4520	.28619	<.001	1.4506	.28635	<.001
.23	1.4759	.29846	<.001	1.4748	.29803	<.001
.24	1.4944	.31483	<.001	1.4944	.31549	<.001
.25	1.4905	.34680	<.001	1.4913	.34780	<.001
.26	1.4698	.37677	<.001	1.4702	.37626	<.001
.27	1.2205	.45165	.001	1.2202	.45322	.001
.28	1.1829	.48707	.006	1.1847	.49041	.006
.29	1.1403	.50749	.041	1.1400	.50705	.042
.30	1.0376	.47474	.553	1.0361	.47162	.566

small-worldness) and the three composite behavioral measurements in the dyslexic group are shown in Table 3. In the density weighted network, the correlations between literacy skill and four network parameters were significant, including CC (r (25) = .689, p = .0005 < FDR-corrected q^* = .0028), LE (r (25) = .701, p = .0004 < FDR-corrected q^* = .0014), T (r (25) = .623, p = .0025 < FDR-corrected q^* = .0056) and GE (r (25) = .687, p = .0006 < FDR-corrected q^* = .0042), as shown in Figure 4. For the number-of-streamline weighted network, CC (r (26) = −.502, p = .0173), LE (r (26) = −.538, p = .0097), T (r (26) = −.481, p = .0234), and GE

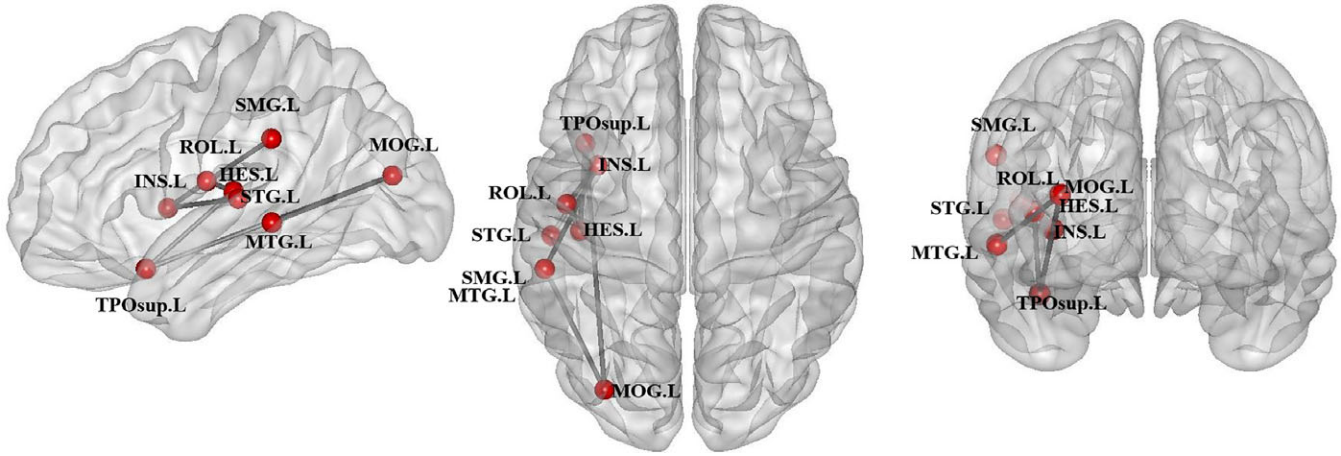

FIGURE 2 Abnormalities in a number-of-streamline weighted brain subnetwork in developmental dyslexia, identified using network-based statistics (NBS). The subnetwork consists of a central cluster of eight nodes and seven edges located in the left occipito-temporo-parietal lobe. L, left; TPOsup, superior temporal pole; MOG, middle occipital gyrus; MTG, middle temporal gyrus; STG, superior temporal gyrus; INS, insula; HES, Heschl's gyrus; ROL, Rolandic operculum; SMG, supramarginal gyrus

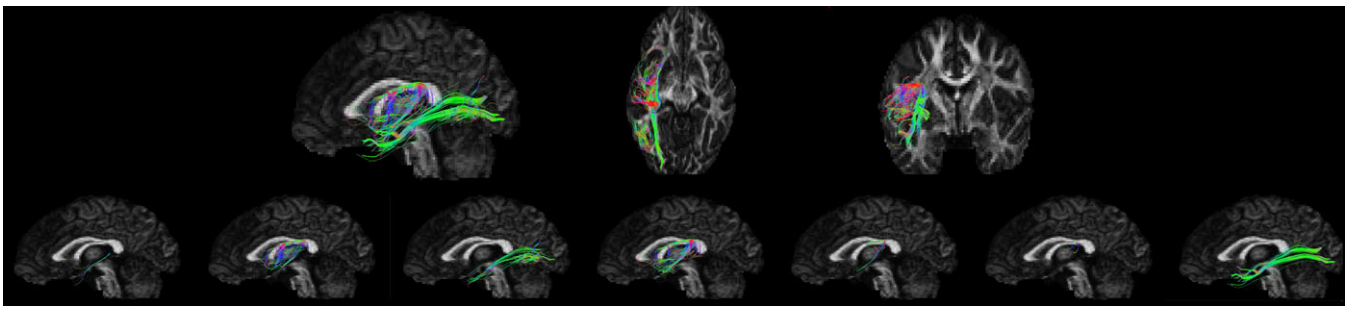

FIGURE 3 The number-of-streamline weighted subnetwork from one representative control child. The top of the figure exhibits the subnetwork. Each of the seven edges in the subnetwork were extracted separately as shown on the bottom of the figure (from left to right: The connections between the left superior temporal pole and the left Heschl's gyrus, the connections between the left insula and the left Rolandic operculum, left middle temporal gyrus and the left middle occipital gyrus, the connections between the left superior temporal gyrus and the left insula, the connections between left insula and the left supramarginal gyrus, the connections between the left Heschl's gyrus and the left Rolandic operculum, and the connection between the left middle occipital gyrus and the left temporal pole)

(r (26) = −.532, p = .0108) showed trend of negative correlation with phonological ability, but they did not survive FDR correction. No significant group difference or network-behavior correlations were found on the number-of-streamline weighted network.

3.5 | Added value of network parameters relative to white matter pathway

As the correlations between literacy skill and four network parameters in the density weighted network were significant, hierarchical multiple regression analyses with literacy skill as dependent variable were further performed. Regression analyses results are presented in Table 4. Gender, age, parental education, and mean global FA together explained 45.3% of the variance in literacy skill (model 1). The LI of IFOF and SLF II significantly explained an additional 25.5% of the variance (model 2). Adding graph theoretical measures significantly increased the explained variance in literacy skill, by 7.2% for clustering coefficient (p = .031), 7.2% for local efficiency (p = .030), by 5.5% for transitivity (p = .062), and by 6.5% for global efficiency (p = .041).

4 | DISCUSSION

The present study investigated white matter network deficits in developmental dyslexia. For the first time, we demonstrated that developmental dyslexia involves widely distributed white matter deficits at the brain-network level. Network topological properties correlated with literacy skills in dyslexia and explained additional variance of the literacy ability in dyslexic children beyond previously established white matter abnormalities.

The first important finding was from the network-based statistics (NBS) analysis. Using NBS, we found that dyslexic children showed fewer connections within an integrated and widespread left hemisphere network including Rolandic operculum, insula, supramarginal gyrus, superior temporal pole, middle occipital gyrus, middle temporal gyrus, superior temporal gyrus, and Heschl's gyrus, compared with matched healthy controls. The connectivity of this local network as indexed by FA was also lower in dyslexic children as compared to control children. Although it emerged from an unbiased whole brain analysis, this left hemisphere subnetwork is largely consistent with widely accepted notions about the neural basis of reading and regional brain alterations in dyslexia (Jobard,

TABLE 3 Pearson partial correlation coefficients (controlled for gender, age, parental education, and mean global FA) between behavioral measures and network parameters in the group of dyslexic children

Correlations between reading performance number-of-streamline weighted network							
	N	*r* (*p*)					
		Clustering coefficient	Local efficiency	Transitivity	Global efficiency	Betweenness centrality	Strength
Literacy ability	25	−.158 (.4930)	−.180 (.4343)	−.138 (.5502)	−.189 (.4120)	−.006 (.9806)	−.208 (.3664)
Phonological ability	26	−.502 (.0173)*	−.538 (.0097)*	−.481 (.0234)*	−.532 (.0108)*	−.039 (.8637)	−.155 (.4924)
Rapid automatic naming	26	.007 (.9753)	.044 (.8470)	.014 (.9510)	.056 (.8041)	.102 (.6501)	.265 (.2333)
Correlations between reading performance density weighted network							
	N	*r* (*p*)					
		Clustering coefficient	Local efficiency	Transitivity	Global efficiency	Betweenness centrality	Strength
Literacy ability	25	**.689 (.0005)****	**.701 (.0004)****	**.623 (.0025)****	**.687 (.0006)****	−.253 (.2694)	.121 (.6017)
Phonological ability	26	.353 (.1069)	.332 (.1420)	.297 (.1799)	.282 (.2036)	−.274 (.2180)	.172 (.4452)
Rapid automatic naming	26	−.231 (.3010)	−.244 (.2728)	−.169 (.4534)	−.221 (.3239)	.182 (.4180)	−.114 (.6128)

*$p < .05$, **$q < 0.05$ (surviving FDR correction).

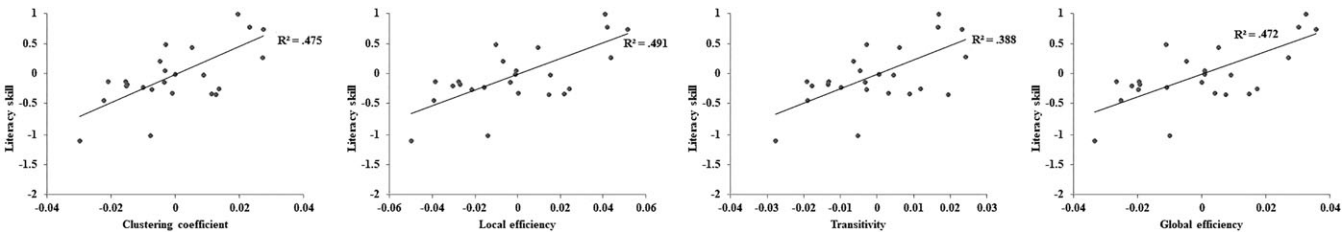

FIGURE 4 Correlations between literacy skills and four density-weighted network topological parameters (clustering coefficient, local efficiency, transitivity, and global efficiency) in dyslexic children

TABLE 4 Explained variance in literacy skill (average z-score of spelling and word reading accuracy) in the group of dyslexic children by white matter pathway markers[a] and network parameters[b]. **$p < .01$, *$p < .05$, #$p < .10$

Model	Independent variables	R^2	ΔR^2	*p*
Literacy skill				
1	Age, gender, parental education, global FA	.453	.453	.013**
2	Model 1 + LI of IFOF and SLF II	.708	.255	.004**
3a[a]	Model 2 + clustering coefficient	.780	.072	.031*
3b[a]	Model 2 + local efficiency	.780	.072	.030*
3c[a]	Model 2 + transitivity	.763	.055	.062#
3d[a]	Model 2 + global efficiency	.773	.065	.041*

Abbreviations: IFOF, inferior frontal-occipital fasciculus; SLF, superior longitudinal fasciculus.
[a] Model 3 includes only those network parameters that were significantly correlated with word reading/spelling accuracy as shown in Table 2.
[b] White matter pathway markers that were significantly correlated with word reading/spelling accuracy from Zhao et al. (2016) were controlled and included in Model 2.
[c] The difference in explained change of variance (ΔR^2) between the model and the previous model and the corresponding *p* value are given.

Crivello, & Tzourio-Mazoyer, 2003; Sandak, Mencl, Frost, & Pugh, 2004; Schlaggar & McCandliss, 2007; Vandermosten, Boets, Poelmans, et al., 2012; Zhao et al., 2016). This disrupted network includes the two main pathways understood to underlie speech and reading processing (for reviews see Hickok & Poeppel, 2007; Vandermosten, Boets, Wouters, & Ghesquiere, 2012). One is the dorsal pathway, which is centered on language-related regions including key regions for auditory processing and phonological processing including inferior frontal regions (ROL), temporal auditory cortex (HES, STG), and multimodal temporo-parietal regions (SMG) [for a review see Vandermosten, Boets, Wouters, & Ghesquiere, 2012]. These regions are notably connected by the arcuate fasciculus (Catani & Thiebaut de Schotten, 2008), a key bundle connecting anterior and posterior language regions.

The other pathway is in the ventral network, including tracts connecting the left-middle occipital gyrus and the left-superior temporal pole. This ventral network overlaps with the inferior longitudinal fasciculus (Catani & Thiebaut de Schotten, 2008). Although few studies have reported abnormalities in dyslexia in the inferior longitudinal fasciculus (Yeatman, Dougherty, Ben-Shachar, & Wandell, 2012), the current finding corroborates previous functional and structural imaging

studies that have reported abnormal function during word form recognition (Dehaene & Cohen, 2011; Price & Devlin, 2011) and atypical gray matter geometry in the occipital-temporal region in dyslexia (Altarelli et al., 2013; Richardson & Price, 2009). In summary, our NBS results revealed a deficit in a subnetwork, which included both dorsal and ventral connections in dyslexic children.

The second important finding is the correlation between whole brain network topological properties (CC, LE, GE, and T) and literacy skill. Network parameter alterations in the dyslexic group were related to behavioral measures of literacy. Thus, the white matter network topological properties we observed may represent neural correlates of reading ability.

Most previous studies in DTI have suggested correlations between literacy skills and white matter connectivity in specific white matter regions (Carter et al., 2009; Deutsch et al., 2005; Klingberg et al., 2000) or specific white matter pathways (Vandermosten, Boets, Poelmans, et al.,2012; Zhao et al., 2016). In the present study, we found for the first time that disconnection of white matter is associated with literacy skills not only in specific white matter regions or pathways but also in whole-brain white matter network properties. According to graph theory, the four parameters can be categorized into two types: integration and segregation. GE is a measure of integration, describing the ability to rapidly communicate among distributed brain regions (Latora & Marchiori, 2001; Rubinov & Sporns, 2010). Thus, positive correlation between GE and literacy skills in dyslexics indicates that less efficient global connectivity among long-range pathways leading to reduced literacy skills in dyslexic children might be caused by less integration of communication between distant regions. LE, CC, and T are measures of segregation, demonstrating the capacity for specialized processing within densely interconnected brain regions (Rubinov & Sporns, 2010). Lower CC, LE, and T are equivalent to less densely connected clusters, which suggests reduced functional segregation of brain regions. Therefore, positive correlation between CC, LE, and T and literacy skills in dyslexics indicates that less independent clusters leading to worse literacy skills in dyslexic children might result from reduced functional segregation within the brain of dyslexic individuals.

Results from hierarchical multiple regression analyses suggest that network measures provide information on literacy ability over and beyond that already provided by previously established white matter tract measures. Indeed, we found that CC, GE, LE, and T explained additional variance in literacy skill beyond the lateralization index of IFOF and SLF II, two white matter pathway measures that Zhao et al. (2016) had found to correlate with literacy skills in the same population. The results indicate that whole-brain network measures may provide important information independent from measurement of specific white matter pathways previously related to dyslexia, and that abnormal whole brain white matter network organization is related to word reading/spelling abilities in dyslexia.

Finally, white matter connection measure in the temporo-parietal local white matter network where dyslexics differ from controls and the global network topological parameters found to be associated with dyslexics' literacy skills may both have genetic origins. Previous studies have consistently shown that genetic factors could affect both white matter volume and local connectivity between different brain regions. For example, dyslexia susceptibility genes (DYX1C1, DCDC2, KIAA0319), which have been implicated in neuronal migration, were associated with white matter volume and its development in left temporo-parietal regions (Darki, Peyrard-Janvid, Matsson, Kere, & Klingberg, 2012; Darki, Peyrard-Janvid, Matsson, Kere, & Klingberg, 2014). DCDC2 and KIAA0319 were also reported to be highly expressed in the temporal and parietal regions (Meng et al., 2005). It therefore indicates that atypical expression of the dyslexia susceptibility genes may lead to white matter disruption in the left temporo-parietal region. Besides, studies have also revealed genes modulating brain connectivity between different brain regions. For example, a gene SLC2A3 which regulates neural glucose transport (Maher & Simpson, 1994; Maher, Vannucci, & Simpson, 1994; McCall, Van Bueren, Moholt-Siebert, Cherry, & Woodward, 1994) and phonological processing (Roeske et al., 2011) was related to FA of the arcuate fasciculus, a white matter fiber pathway linking Broca's area and Wernicke's area (Skeide et al., 2015). ROBO1, a gene related to axon guidance receptor, was also shown to be related to reading behavior and connectivity (axonal diffusion) of the middle corpus callosum, white matter fiber pathway linking the left hemisphere and the right hemisphere (Sun et al., 2017). In the present study, using NBS we have identified a subnetwork with less white matter streamlines in the dyslexic groups than in the control groups in distributed left temporo-parietal region. The edges of our subnetwork included left arcuate fasciculus, which have been reported to be related to gene SLC2A3. The node of our subnetwork included supramarginal gyrus, which also overlapped with the left temporo-parietal region where Darki et al. found to be associated with dyslexia susceptibility genes (DYX1C1, DCDC2, KIAA0319). Therefore, we speculated that the group differences between dyslexics and controls found in the local temporo-parietal network may have genetic basis to SLC2A3 and DYX1C1, DCDC2, and KIAA0319, although these speculations might still require future examinations. In addition, we also expect that the more global network topological parameters might also have genetic origins with dyslexia susceptibility genes (DYX1C1, DCDC2, KIAA0319) and genes associated with phonological abilities and reading skills (e.g., SLC2A3 and ROBO1), as we found that the global network topological properties were associated with dyslexics' literacy skills. All these expectations should be tested systematically before making firm conclusions. Nevertheless, our results suggest future directions for investigating the genetic origins of white matter network organization and properties in developmental dyslexia.

It should be noted that the significant results from NBS analysis were for the number-of-streamline weighted network but the significant global network-behavior correlations were based on the density weighted network. This discrepancy between two different network analysis methods and two edge-weighted network may be due to (1) the nature of the two different network analysis methods, and (2) the differences of the edge definitions of the two edge-weighted network. First, NBS and graph theoretical analysis are based on different statistical methods and reflect different network properties. NBS applied a set of *t* tests to examine group differences on every edge of the network. Any significant group difference on the subnetwork was based on the exact connectivity of the white matter pathways in the subnetwork. Therefore, NBS reflects local connectivity of the network. In contrast, graph theory analysis quantified the whole-brain topological structure of the white matter network, therefore reflecting

more global and complex network properties than the simple connectivity of specific edges in the network. Second, the edges in the streamline weighted network and the density weighted network reflect different characteristics of the connectivity. The edge in the streamline weighted network is the exact number of streamlines between two brain regions, whereas the edge in the density weighted network divides streamline number by the total volume of two brain regions, which potentially normalizes the sizes and connections of brain regions. Therefore, the streamline weighted edges would be more sensitive to reflect the local differences in a subnetwork. Comparatively, density weighted edges would be more suitable for evaluating whole brain network properties, as at the global whole brain level, it is necessary to normalize the streamline number with brain volume to standardize each edge. To sum up, results on networks with streamline-weighted values in NBS and density-weighted values in graph theoretical analysis might reflect different types of white matter connectivity at local and global levels biased by streamline-weighted and density-weighted edge definitions. Our findings of group differences in streamline weighted local network by NBS indicate that the network-neuropathology of dyslexia might be more sensitive at the local level network structure, which is also consistent with previous studies (e.g., Finn et al., 2014; Qi et al., 2016). Our results of brain-behavior correlations in dyslexia found by graph theoretical analysis in global density-weighted network seem to indicate that the global level network parameters might be more sensitive to account for the behavioral variations in dyslexia, which requires future validations of course.

It should also be acknowledged that although the network analysis procedure that we used in the present study for studying dyslexia was the widely used procedure for white network analysis, some drawbacks existed in the procedure. First, the AAL parcellation that we used for defining nodes was a standard practice in the field of network analysis. However, the AAL template is underpowered since gyral parcellation is not related to functional parcellation. Future studies might consider using functional parcellated template to define nodes for network analysis, which might help understand the reading-specific network deficits in dyslexia. Second, the core measurements from the current standard white matter network analysis procedure are number of streamlines, which are criticized as a measure of connectivity strength, but can be seen as a surrogate for connectivity strength measure. Future studies might explore other more transparent white matter connectivity measures such as anisotropy in the network analysis of dyslexia.

5 | CONCLUSIONS

This study was the first study identifying alterations of white matter connectivity in whole-brain connectome level. The findings demonstrate that white matter connections in a local left occipito-temporo-parietal network are disrupted in developmental dyslexia. Furthermore, global white matter network properties generated based on graph theoretical analyses were correlated with literacy skills in dyslexia, and added to the prediction of literacy skills beyond the contributions of specific white matter tracts known from previous work to be related to developmental dyslexia.

ACKNOWLEDGMENTS

This study was supported by the Youth Fund for Humanities and Social Sciences Research of the Ministry of Education (17XJC190010), the General Project (Youth) of Shaanxi Natural Science Basic Research Program (2018JQ8015), and the Fundamental Research Funds for the Central Universities (GK201702011) to Jingjing Zhao. This study was also funded by Agence Nationale de la Recherche (contracts ANR-06-NEURO-019-01, ANR-11-BSV4-014-01, ANR-10-LABX-0087, ANR-11-0001-02 PSL*) and Ecole des Neurosciences de Paris. We thank Jessica Dubois, Michel Thiebaut de Schotten, Catherine Billard, Joël Fluss, Ghislaine Dehaene-Lambertz, Nadège Villiermet, Stéphanie Iannuzzi for their collaboration, and the technical and clinical staff at Hôpital Bicêtre and Neurospin. We appreciate the efforts of all children and their families who participated in this study. We especially thank Michel Thiebaut de Schotten for valuable comments.

CONFLICT OF INTERESTS

None of the authors has conflict of interests.

ORCID

Jingjing Zhao https://orcid.org/0000-0001-9000-6227

REFERENCES

Achenbach, T. M. (2001). *Child behavior checklist. Burlington: ASEBA* (pp. 546–552). New York, NY: Springer New York.

Ahuja, R. K., Magnanti, T. L., & Orlin, J. B. (1993). Network flows: Theory, algorithms, and applications. *Journal of the Operational Research Society*, *45*, 791–796.

Altarelli, I., Monzalvo, K., Iannuzzi, S., Fluss, J., Billard, C., Ramus, F., & Dehaene-Lambertz, G. (2013). A functionally guided approach to the morphometry of occipitotemporal regions in developmental dyslexia: Evidence for differential effects in boys and girls. *Journal of Neuroscience*, *33*, 11296–11301.

Ball, G., Aljabar, P., Zebari, S., Tusor, N., Arichi, T., Merchant, N., … Edwards, A. D. (2014). Rich-club organization of the newborn human brain. *Proceedings of the National Academy of Sciences of the United States of America*, *111*, 7456–7461.

Basser, P. J. (1995). Inferring microstructural features and the physiological state of tissues from diffusion-weighted images. *NMR in Biomedicine*, *8*, 333–344.

Basser, P. J., Mattiello, J., & Lebihan, D. (1994). MR diffusion tensor spectroscopy and imaging. *Biological Journal*, *66*, 259–267.

Batalle, D., Hughes, E. J., Zhang, H., Tournier, J. D., Tusor, N., Aljabar, P., … Counsell, S. J. (2017). Early development of structural networks and the impact of prematurity on brain connectivity. *NeuroImage*, *149*, 379–392.

Benjamini, Y., & Hochberg, Y. (1995). Controlling the false discovery rate: A practical and powerful approach to multiple testing. *Journal of Royal Statistical Society B*, *57*, 289–300.

Boets, B., Beeck, H. O.d., Vandermosten, M., Scott, S. K., Gillebert, C. R., Mantini, D., … Ghesquière, P. (2013). Intact but less accessible phonetic representations in adults with dyslexia. *Science*, *342*, 1251–1254.

Bosse, M. L., & Valdois, S. (2009). Influence of the visual attention span on child reading performance: A cross-sectional study. *Journal of Research in Reading*, *32*, 230–253.

Brambati, S. M., Termine, C., Ruffino, M., Danna, M., Lanzi, G., Stella, G., … Perani, D. (2006). Neuropsychological deficits and neural dysfunction in familial dyslexia. *Brain Research*, *1113*, 174–185.

Carter, J. C., Lanham, D. C., Cutting, L. E., Clements-Stephens, A. M., Chen, X., Hadzipasic, M., … Kaufmann, W. E. (2009). A dual DTI approach to analyzing white matter in children with dyslexia. *Psychiatry Research*, *172*, 215–219.

Catani, M., & Thiebaut de Schotten, M. (2008). A diffusion tensor imaging tractography atlas for virtual in vivo dissections. *Cortex*, *44*, 1105–1132.

Cohen, L., & Dehaene, S. (2004). Specialization within the ventral stream: The case for the visual word form area. *NeuroImage*, *22*, 466–476.

Cohen, L., Dehaene, S., Naccache, L., Lehéricy, S., Dehaenelambertz, G., Hénaff, M. A., & Michel, F. (2000). The visual word form area: Spatial and temporal characterization of an initial stage of reading in normal subjects and posterior split-brain patients. *Brain A Journal of Neurology*, *123*Pt 2, 291–307.

Darki, F., Peyrard-Janvid, M., Matsson, H., Kere, J., & Klingberg, T. (2012). Three dyslexia susceptibility genes, DYX1C1, DCDC2, and KIAA0319, affect temporo-parietal white matter structure. *Biological Psychiatry*, *72*, 671–676.

Darki, F., Peyrard-Janvid, M., Matsson, H., Kere, J., & Klingberg, T. (2014). DCDC2 polymorphism is associated with left temporoparietal gray and white matter structures during development. *Journal of Neuroscience*, *34*, 14455–14462.

Dehaene, S., & Cohen, L. (2011). The unique role of the visual word form area in reading. *Trends in Cognitive Sciences*, *15*, 254–262.

Deutsch, G. K., Dougherty, R. F., Bammer, R., Siok, W. T., Gabrieli, J. D. E., & Wandell, B. (2005). Children's reading performance is correlated with white matter structure measured by diffusion tensor imaging. *Cortex*, *41*, 354–363.

Drakesmith, M., Caeyenberghs, K., Dutt, A., Lewis, G., David, A. S., & Jones, D. K. (2015). Overcoming the effects of false positives and threshold bias in graph theoretical analyses of neuroimaging data. *NeuroImage*, *118*, 313–333.

Dubois, J., Poupon, C., Lethimonnier, F., & Bihan, D. L. (2006). Optimized diffusion gradient orientation schemes for corrupted clinical DTI data sets. *Magnetic Resonance Materials in Physics, Biology and Medicine*, *19*, 134–143.

Epelbaum, S., Pinel, P., Gaillard, R., Delmaire, C., Perrin, M., & Dupont, S. (2008). Pure alexia as a disconnection sydrome: New diffusion imaging evidence for an old concept. *Cortex*, *44*, 962–974.

Fawcett, A. J., & Nicolson, R. (2007). Dyslexia, learning, and pedagogical neuroscience. *Developmental Medicine & Child Neurology*, *49*, 306–311.

Finn, E. S., Shen, X., Holahan, J. M., Scheinost, D., Lacadie, C., Papademetris, X., … Constable, R. T. (2014). Disruption of functional networks in dyslexia: A whole-brain, data-driven analysis of connectivity. *Biological Psychiatry*, *76*, 397–404.

Giraud, A.-L., & Ramus, F. (2013). Neurogenetics and auditory processing in developmental dyslexia. *Current Opinion in Neurobiology*, *23*, 37–42.

Hickok, G., & Poeppel, D. (2007). The cortical organization of speech processing. *Nature Reviews Neuroscience*, *8*, 393–402.

Hoeft, F., Hernandez, A., McMillion, G., Taylor-Hill, H., Martindale, J. L., & Meyler, A. (2006). Neural basis of dyslexia: A comparison between dyslexic and nondyslexic children equated for reading ability. *The Journal of Neuroscience*, *26*, 10700–10708.

Hoeft, F., Meyler, A., Hernandex, A., Juel, C., Taylor-Hill, H., & Martindale, J. L. (2007). Functional and morphometric brain dissociation between dyslexia and reading ability. *Proceedings of the National Academy of Sciences of the United States of America*, *104*, 4234–4239.

Horwithz, B., Rumsey, J. M., & Donohue, B. C. (1998). Functional connectivity of the angular gyrus in normal reading and dyslexia. *Proceedings of the National Academy of Sciences of the United States of America*, *95*, 8939–8944.

Hosseini, S. M. H., Black, J. M., Soriano, T., Bugescu, N., Martinez, R., Raman, M. M., … Hoeft, F. (2013). Topological properties of large-scale structural brain networks in children with familial risk for reading difficulties. *NeuroImage*, *71*, 260–274.

Humphries, M. D., & Gurney, K. (2008). Network 'small-world-ness': A quantitative method for determining canonical network equivalence. *PLoS One*, *3*, e0002051.

Jacquier-Roux, M., Valdois, S., & Zorman, M. (2005). *Odédys: Outil de dépistage des dyslexiques. Version 2*. Grenoble: Laboratoire Cognisciences.

Jenkinson, M., Beckmann, C. F., Behrens, T. E., Woolrich, M. W., & Smith, S. M. (2012). FSL. *NeuroImage*, *62*, 782–790.

Jobard, G., Crivello, F., & Tzourio-Mazoyer, N. (2003). Evaluation of the dual route theory of reading: A metanalysis of 35 neuroimaging studies. *NeuroImage*, *20*, 693–712.

Klingberg, T., Hedehus, M., Temple, E., Salz, T., Gabriell, J. D. E., Moseley, M. E., & Poldrack, R. A. (2000). Microstructure of temporo-parietal white matter as a basis for reading ability: Evidence from diffusion tensor magnetic resonance imaging. *Neuron*, *25*, 493–500.

Korgaonkar, M. S., Fornito, A., Williams, L. M., & Grieve, S. M. (2014). Abnormal structural networks characterize major depressive disorders: A connectome analysis. *Biological Psychiatry*, *76*, 567–575.

Latora, V., & Marchiori, M. (2001). Efficient behavior of small-world networks. *Physical Review Letters*, *87*, 1–4.

Leemans, A., Jeurissen, B., Sijbers, J., Jones, D.K. (2009) *ExploreDTI: A graphical toolbox for processing, analyzing, and visualizing diffusion MR data*. Proceedings of the 17th Scientific Meeting, International Society for Magnetic Resonance in Medicine, Honolulu, HI, p. 3537.

Lefavrais, P. (1967). *Test de l'Alouette* (2nd ed.). Paris: Editionsdu Centre de Psychologie Appliquée.

Lyon, G. R., Shaywitz, S. E., & Shaywitz, B. A. (2003). A definition of dyslexia. *Annals of Dyslexia*, *53*, 1–14.

Maher, F., & Simpson, I. A. (1994). Modulation of expression of glucose transporters GLUT3 and GLUT1 by potassium and N-methyl-d-aspartate in cultured cerebellar granule neurons. *Molecular and Cellular Neuroscience*, *5*, 369–375.

Maher, F., Vannucci, S., & Simpson, I. (1994). Glucose transporter proteins in brain. *The FASEB Journal*, *8*, 1003–1011.

Makris, N., Goldstein, J., Kennedy, D., Hodge, S., Caviness, V., Faraone, S., … Seidman, L. (2006). Decreased volume and total anteiror insular lobule in schizophrenia. *Schizophrenia Research*, *83*(2–3), 151–155.

Martinet, C., & Valdois, S. (1999). Learning to spell words: Difficulties in developmental surface dyslexia. *L'Année Psychologique*, *99*, 577–592.

McCall, A. L., Van Bueren, A. M., Moholt-Siebert, M., Cherry, N. J., & Woodward, W. R. (1994). Immunohistochemical localization of the neuron-specific glucose transporter (GLUT3) to neuropil in adult rat brain. *Brain Research*, *659*, 292–297.

Meng, H., Smith, S. D., Hager, K., Held, M., Liu, J., Olson, R. K., … Gruen, J. R. (2005). DCDC2 is associated with reading disability and modulates neuronal development in the brain. *Proceedings of the National Academy of Sciences of the United States of America*, *102*, 17053–17058.

Meunier, D., Achard, S., Morcom, A., & Bullmore, E. (2009). Age-related changes in modular organization of human brain functional networks. *NeuroImage*, *44*, 715–723.

Niogi, S. N., & McCandliss, B. D. (2006). Left lateralized white matter microstructure accounts for individual differences in reading ability and disability. *Neuropsychologia*, *44*, 2178–2188.

Paulesu, E., Danelli, L., & Berlingeri, M. (2014). Reading the dyslexic brain: Multiple dysfunctional routes revealed by a new meta-analysis of PET and fMRI activation studies. *Frontiers in Human Neuroscience*, *8*, 1–20.

Paulesu, E., Frith, U., Snowling, M., Gallagher, A., Morton, J., Frackowiak, R. S. J., & Frith, C. D. (1996). Is developmental dyslexia a disconnection syndrome? Evidence from PET scanning. *Brain*, *119*, 143–157.

Plaza, M., & Robert-Jahier, A. M. (2006). *DRA: Test dénomination rapide enfants*. Magny-en-Vexin: Adeprio Diffusion.

Price, C. J., & Devlin, J. T. (2011). The interactive account of ventral occipitotemporal contributions to reading. *Trends in Cognitive Sciences*, *15*, 246–253.

Pugh, K. R., Mencl, W. E., Shaywitz, B. A., Shaywitz, S. E., Fulbright, R. K., Constable, R. T., … Gore, J. C. (2000). The angular gyrus in developmental dyslexia: Task-specific differences in functional connectivity within posterior cortex. *Psychological Science*, *11*, 51–56.

Qi, T., Gu, B., Ding, G., Gong, G., Lu, C., Peng, D., … Liu, L. (2016). More bilateral, more anterior: Alterations of brain organization in the large-scale structural network in Chinese dyslexia. *NeuroImage*, *124*, 63–74.

Reijmer, Y. D., Leemans, A., Caeyenberghs, K., Heringa, S. M., Koek, H. L., & Biessels, G. J. (2013). Disruption of cerebral networks and cognitive impairment in Alzheimer disease. *Neurology*, *80*, 1370–1377.

Richards, T., Stevenson, J., Crouch, J., Johnson, L. C., Maravilla, K., Stock, P., … Berninger, V. (2008). Tract-based spatial statistics of diffusion tensor imaging in adults with dyslexia. *American Journal of Neuroradiology*, *29*, 1134–1139.

Richardson, F. M., & Price, C. J. (2009). Structural MRI studies of language function in the undamaged brain. *Brain Structure & Function*, *213*, 511–523.

Rimrodt, S. L., Clements-Stephens, A. M., Pugh, K. R., Courtney, S. M., Gaur, P., Pekar, J. J., & Cutting, L. E. (2009). Functional MRI of sentence comprehension in children with dyslexia: Beyond word recognition. *Cerebral Cortex*, *19*, 402–413.

Roeske, D., Ludwig, K., Neuhoff, N., Becker, J., Bartling, J., Bruder, J., … Hoffmann, P. (2011). First genome-wide association scan on neurophysiological endophenotypes points to trans-regulation effects on SLC2A3 in dyslexic children. *Molecular Psychiatry*, *16*, 97–107.

Roine, U., Roine, T., Salmi, J., Wendt, T. N., Tani, P., Leppämäki, S., … Sams, M. (2015). Abnormal wiring of the connectome in adults with high-functioning autism spectrum disorder. *Molecular Autism*, *6*, 11.

Rubinov, M., & Sporns, O. (2010). Complex network measures of brain connectivity: Uses and interpretations. *NeuroImage*, *52*, 1059–1159.

Saksida, A., Iannuzzi, S., Bogliotti, C., Chaix, Y., Démonet, J. F., Bricout, L., … Ramus, F. (2016). Phonological skills, visual attention span, and visual stress in developmental dyslexia. *Developmental Psychology*, *52*, 1503–1516.

Sandak, R., Mencl, W. E., Frost, S. J., & Pugh, K. R. (2004). The neurobiological basis of skilled and impaired reading: Recent findings and new directions. *Scientific Studies of Reading*, *8*, 273–292.

Schlaggar, B. L., & McCandliss, B. D. (2007). Development of neural systems for reading. *Annual Review of Neuroscience*, *30*, 475–503.

Schurz, M., Wimmer, H., Richlan, F., Ludersdorfer, P., Klackl, J., & Kronbichler, M. (2015). Resting-state and task-based functional brain connectivity in developmental dyslexia. *Cerebral Cortex*, *25*, 3502–3514.

Shaywitz, B. A., Shaywitz, S. E., Pugh, K. R., Mencl, W. E., Fulbright, R. K., Skudlarski, P., … Gore, J. C. (2002). Disruption of posterior brain systems for reading in children with developmental dyslexia. *Biological Psychiatry*, *52*, 101.

Shaywitz, S. E., & Shaywitz, B. A. (2005). Dyslexia (specific reading disability). *Biological Psychiatry*, *57*, 1301–1309.

Shaywitz, S. E., Shaywitz, B. A., Fletcher, J., & Escobar, M. (1990). Prevalence of reading disability in boys and girls. *Journal of the American Medical Association*, *264*, 998–1002.

Siegel, L. S. (2006). Perspectives on dyslexia. *Paediatrics & Child Health*, *11*, 581–587.

Skeide, M. A., Kirsten, H., Kraft, I., Schaadt, G., Müller, B., Neef, N., … Friederici, A. D. (2015). Genetic dyslexia risk variant is related to neural connectivity patterns underlying phonological awareness in children. *NeuroImage*, *118*, 414–421.

Sporns, O. (2014). Contributions and challenges for network models in cognitive neuroscience. *Nature Neuroscience*, *17*, 652–660.

Sprenger-Charolles, L., Béchennec, D., Colé, P., & Kipffer-Piquard, A. (2005). French normative data on reading and related skills from EVALEC, a new computerized battery of tests. End grade 1, grade 2, grade 3, and grade 4. *Revue Europeene de Psychologie Appliquee*, *55*, 157–186.

Steinbrink, C., Vogt, K., Kastrup, A., Muller, H.-P., Juengling, F. D., Kassubek, J., & Riecker, A. (2008). The contribution of white and gray matter differences to developmental dyslexia: Insight from DTI and VBM at 3.0 T. *Neuropsychologia*, *46*, 3170–3178.

Sun, X., Song, S., Liang, X., Xie, Y., Zhao, C., Zhang, Y., … Gong, G. (2017). *ROBO1 polymorphisms, callosal connectivity, and reading skills. Human brain mapping*, 38, 2616–2626.

Tournier, J.-D., Calamante, F., & Connelly, A. (2007). Robust determination of the fibre orientation distribution in diffusion MRI: Non-negativity constrained super-resolved spherical deconvoluton. *NeuroImage*, *35*, 1459–1472.

Tzourio-Mazoyer, N., Landeau, B., Papathanassiou, D., Etard, F. C. O., Delcroix, N., Mazoyer, B., & Joliot, M. (2002). Antomated anatomical labeling of activations in SPM using a macroscopic anatomical parcellation of the MNI MRI single-subject brain. *NeuroImage*, *15*, 273–289.

van den Heuvel, M. P., Stam, C. J., Kahn, R. S., & Hulshoff Pol, H. E. (2009). Efficiency of functional brain networks and intellectual performance. *Journal of Neuroscience*, *29*, 7619–7624.

Vandermosten, M., Boets, B., Poelmans, H., Sunaert, S., Wouters, J., & Ghesquière, P. (2012). A tractography study in dyslexia: Neuroanatomic correlates of orthographic, phonological and speech processing. *Brain*, *135*, 935–948.

Vandermosten, M., Boets, B., Wouters, J., & Ghesquiere, P. (2012). A qualitative and quantitative review of diffusion tensor imaging studies in reading and dyslexia. *Neuroscience & Biobehavioral Reviews*, *36*, 1532–1552.

Wang, T., Shi, F., Jin, Y., Yap, P.-T., Wee, C.-Y., Zhang, J., Yang, C., Li, X., Xiao, S., Shen, D. (2015) Multilevel deficiency of white matter connectivity networks in Alzheimer's disease: A diffusion MRI study with DTI and HARDI models. *Neural Plasticity*, 2016, 1–15.

Watts, D. J., & Strogatz, S. H. (1998). Collective dynamics of 'small-world' networks. *Nature*, *393*, 440–442.

Wechsler, D. (2005). *WISC-IV: Echelle d'Intelligence de Wechsler pour Enfants - Quatrième edition*. Paris: Editions du Centre de Psychologie Appliquee.

Xia, M., Wang, J., & He, Y. (2013). BrainNet viewer: A network visualization tool for human brain connectomics. *PLoS One*, *8*, 1–15.

Yeatman, J. D., Dougherty, R. F., Ben-Shachar, M., & Wandell, B. A. (2012). Development of white matter and reading skills. *Proceedings of the National Academy of Sciences of the United States of America*, *109*, 3045–3053.

Zalesky, A., Fornito, A., & Bullmore, E. T. (2010). Network-based statistic: Identifying differences in brain networks. *NeuroImage*, *53*, 1197–1207.

Zhang, J., Wang, J., Wu, Q., Kuang, W., Huang, X., He, Y., & Gong, Q. (2011). Disrupted brain connectivity networks in drug-naive, first-episode major depressive disorder. *Biological Psychiatry*, *70*, 334–342.

Zhao, J., Schotten, M. T., Altarelli, I., Dubois, J., & Ramus, F. (2016). Altered hemisphperic lateralization of white matter pathways in developmental dyslexia: Evidence from spherical deconvolution tractography. *Cortex*, *76*, 51–62.

Zhou, W., Xia, Z., Bi, Y., & Shu, H. (2015). Altered connectivity of the dorsal and ventral visual regions in dyslexic children: A resting-state fMRI study. *Frontiers in Human Neuroscience*, *9*, 1–10.

SUPPORTING INFORMATION

Additional supporting information may be found online in the Supporting Information section at the end of the article.

How to cite this article: Lou C, Duan X, Altarelli I, Sweeney JA, Ramus F, Zhao J. White matter network connectivity deficits in developmental dyslexia. *Hum Brain Mapp*. 2019;40:505–516. https://doi.org/10.1002/hbm.24390